



Composition and properties of tectosilicate-uranium layers of soil

Cecilio Duarte Alaniz^{a,b}, Eduardo Ordoñez Regil^{a,*}, Guillermo Jesus Cruz Cruz^c,
Jesus Ramirez Torres^{d,†} and José López Monroy^d

^a Departamento de Química, Instituto Nacional de Investigaciones Nucleares, Carretera México-Toluca S/N, La Marquesa, Ocoyoacac, Estado de México, CP 52750, México

^b Facultad de Ciencias, Universidad Autónoma del Estado de México, Unidad Académica del Cerrillo, Piedras Blancas El Cerrillo, Tlachaloya Estado de México, CP 50000, México

^c Departamento de Física, Instituto Nacional de Investigaciones Nucleares, Carretera México-Toluca S/N, La Marquesa, Ocoyoacac, Estado de México, CP 52750, México

^d Acelerador Tandem, Instituto Nacional de Investigaciones Nucleares, Carretera México-Toluca S/N, La Marquesa, Ocoyoacac, Estado de México, CP 52750, México

*Corresponding author at: Departamento de Química, Instituto Nacional de Investigaciones Nucleares, Carretera México-Toluca S/N, La Marquesa, Ocoyoacac, Estado de México, CP 52750, México. Tel.: +52.55.53297200; fax: +52.55.53297301. E-mail address: eduardo.ordonez@inin.gob.mx (E. Ordoñez-Regil)

† In memoriam.

ARTICLE INFORMATION

Received: 07 September 2011

Received in revised form: 09 October 2011

Accepted: 13 October 2011

Online: 31 March 2012

KEYWORDS

Albite

Anorthite

Orthoclase

Surface area

Acidity constants

Potentiometric titrations

ABSTRACT

Structure and superficial properties of tectosilicates found in soils with potential to retain uranium are studied in this work. These tectosilicates are largely available as natural minerals in the soil and are composed mainly by anorthite ($\text{CaAl}_2\text{Si}_2\text{O}_8$), albite ($\text{NaAlSi}_3\text{O}_8$) and orthoclase (KAlSi_3O_8), in which albite has approximately 3 times the content of orthoclase and 2.5 times the content of anorthite. However, anorthite has a double cell structure, which could result in approximately the same sorption effect as albite. The acidity constants calculated with the surface complexation model suggested that the three components have similar amphoteric behavior in presence of high ionic strength ground salt solutions. The composite mineral has a specific surface area of $20.5 \text{ m}^2\text{g}^{-1}$ with site density of $2.8 \text{ sites nm}^{-2}$. These characteristics make this mineral a good candidate for uranium capture.

1. Introduction

Soil has low concentration of uranium, but the continuous use of phosphate fertilizers, which contains uranium, produces progressive increases of this component in agricultural lands and their surrounding groundwater. The uranium contamination can range from an average content of 1 mg/Kg up to 200 mg/Kg [1], which is an undesirable level if it is not controlled. One case of natural self-controlled contamination of uranium was found in the agricultural area of Toluca in Mexico. Areas of this land were fertilized for at least 20 agricultural cycles with concentrated phosphates ($\approx 200 \text{ Kg/Ha}$) and showed an abnormal concentration of uranium in some layers of vadose zones (up to 50 mg/Kg) [2]. Fertilization phosphates permeated down from the surface and the associated uranium was partially retained in one of the lower layers avoiding major dispersion in the groundwater [3]. The layer was composed by tectosilicates, silica and organic matter. In the other layers, silica and organic matter were found in similar composition as this layer, but the uranium and tectosilicate content was much lower.

With the purpose to identify and characterize the mineral components in that vadose zone, this work presents a study of those layers of soil with capacity to retain uranium. The minerals in those layers could have potential application in the remediation of environmental contamination of uranium or in the construction of barriers in deep geological repositories of uranium wastes of nuclear industry [4-10]. Historically, it has

been reported that one absorbent of uranium is hydroxyapatite, although its absorption mechanism is still under discussion [11-12]. Up to now, the studies of such barriers have been focused on the sorption of uranium in zirconium oxides, bentonites, calcareous clays and synthetic phosphates [13-18]. Zirconium oxides have shown absorption of some lanthanides in solution and bentonites (phyllosilicates) have great cation exchange capacity. Studies on other candidates such as calcareous clays are still in progress [19]. One advantage of the vadose minerals studied in this work in the sorption of uranium is that they can be found as natural components in some soils.

In sorption processes, the surface plays a great role in the retention of ions and particles, so the surface of the resulting mineral was studied on the basis that a solid immersed in a liquid solution develops hydroxylated groups ($\equiv\text{SOH}$) due to the interaction of superficial charges with water. The strong dependence of charges on the surface, with respect to pH, and the proton abundance in the solutions are responsible for the amphoteric behavior of materials [20-21]. Thus, the properties studied in this work include amphoteric behavior at the water/mineral interface, site density, acidity constants and distribution of chemical species [22-23].

2. Experimental

Samples of soil were taken in cylinders that penetrate vertically, 180 cm depth, from the surface of an agronomical area that had been fertilized with phosphates during several

agricultural cycles in the Toluca, Mexico area [3]. The soil of the vadose layers was sieved, washed and heated to eliminate the organic matter and to separate minerals. The leaching solution was concentrated and analyzed for uranium by colorimetric methods.

The resulting minerals were analyzed by different techniques. Morphology was studied by means of a Philips XL-30 Scanning Electron Microscope. The specific surface area was quantified with a Quantachrome Autosorb 1 apparatus, operated under Nitrogen atmosphere, with samples in the 35-40 mg interval. The analysis time was 221.9 min and the results were plotted as 20 points BET isotherms.

X-ray diffraction (XRD) was performed in a Co tube Siemens D500 diffractometer to identify species in the extracted minerals. The equilibrium point (zero charge) of negative and positive species is intrinsic to each mineral and depends on the surface site density [1,23,24].

The point of zero charge of the minerals was obtained with mass titration techniques [17,19] with solutions of 10 mL of KNO_3 0.5 M with different solid/water mass ratio: 0.01%, 0.1%, 1%, 5% 10%, 20% and 30%. The suspensions were shaken continuously for 24 hr at 45 rpm and after that, the phases of suspension were separated by centrifuging at 3500 rpm for 15 min. pH of supernatant solutions was measured to calculate the isoelectric point of minerals, which depends on the content of oxides on the surface [20-24].

The surface hydration time was calculated by acid/base potentiometric titrations in a ThermoOrion 720A+ potentiometer with a combined Ag/AgCl electrode. Batches of 2.0 g of solid immersed in 30 mL of 0.5 M potassium nitrate solution were titrated at different contact times of 1, 5, 17, 24 and 72 hours with an agitation speed of 45 rpm. The hydration equilibrium was reached when two similar consecutive titration curves were acquired [7].

The surface site density was estimated by acid-basic titrations of aqueous suspensions. 10.0 g of dried mineral powder was mixed with 100 mL of KNO_3 0.5 M at 303 K. The solution was acidified at pH = 2 with HNO_3 and titrated under Nitrogen atmosphere [25]. A blank solution of the background salt was also titrated. The acid consumption was quantified and the differences between the suspensions and the blank solution were used to obtain the surface sites. The surface acidity constants of the minerals were obtained by fitting the potentiometric titration curve in 0.5 M KNO_3 using the constant capacitance model (CCM), commonly used for high ionic strength solutions in the FITEQL4 code [21].

3. Results and discussion

3.1. Retention of uranium

To study the retention of uranium at different depth from the surface, two kinds of soils were chosen, one non-agricultural land for blank test, and another agricultural land submitted to an intensive fertilization with phosphates. Figure 1 shows the uranium content in the soil at different depth, from 0 to 180 cm. Beyond this depth there was water combined with minerals and soil that modified the tendency of the uranium retention.

On the surface, the content of UO_2 is approximately 31 ppm, which permeates into the soil increasing the uranium content up to 50 ppm in the 30-60 cm segment. This concentration indicates that this layer contains minerals that partially retain uranium. After this segment, the uranium content decreases to 15-20 ppm in the 135-160 cm segment. In non-fertilized soils, the content of UO_2 oscillates between 0-1 ppm, which can be considered the normal uranium content in this soil.

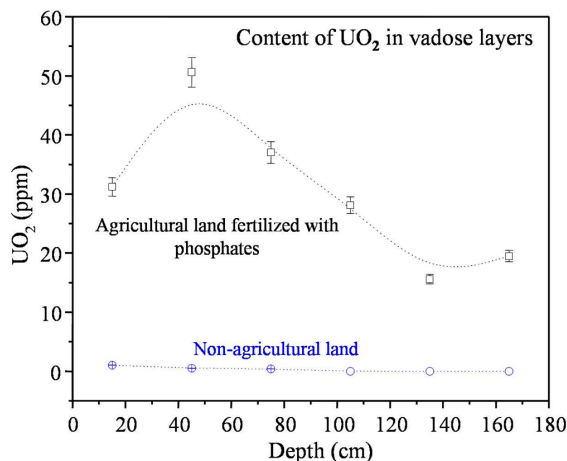


Figure 1. Uranium content in vadose layers at different depth of non-fertilized and fertilized land with phosphates. Note the abnormal concentration of UO_2 at 45 cm depth.

3.2. Morphology of minerals

The layer that retained uranium was located at approximately 30-60 cm depth, so samples of soil in that position were mixed, sieved and washed to remove colloids and soluble salts. After that, the resulting matter reacted with nitric acid and heated up to 800 °C to destroy the residual organic matter. The minerals obtained at the end of this process are shown in Figure 2.

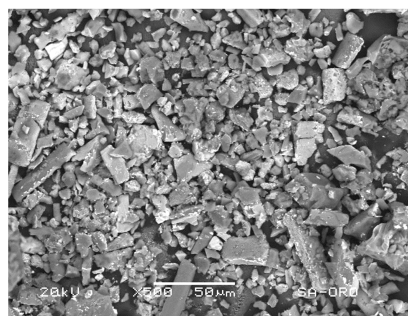


Figure 2. Particles extracted from the vadose layer with capacity to retain uranium.

The image shows that the minerals in the vadose layers are composed of irregular grains with an average length between 5 and 50 μm . The shape and texture of grains suggest that all particles belong to the same mineral, and the size indicates that no colloids or aggregates will be formed in water suspensions.

3.3. Crystallinity

The X-ray diffractogram of vadose minerals in a 2θ scheme is shown in Figure 3. The main diffraction peaks are located at 21.92° , 23.63° , 26.61° , 27.97° and 28.14° . These angles belong to the overlapped crystalline structures of albite, anorthite and orthoclase (JCPDF cards 41-1480, 20-0528, and 31-0966, respectively). There are also other structures containing silicon oxides in quartz forms at 20.82° and 26.21° (JCPDF cards 33-1161).

Figure 4 shows a representation of crystalline cells of albite, orthoclase and anorthite. The first two have similar structures with a different monovalent cation, K^+ or Na^+ , respectively, arranged in single isomorphous cells. However, anorthite has a bivalent cation, Ca^{2+} , in its structure that causes formation of twin cells in c-axis, see Table 1.

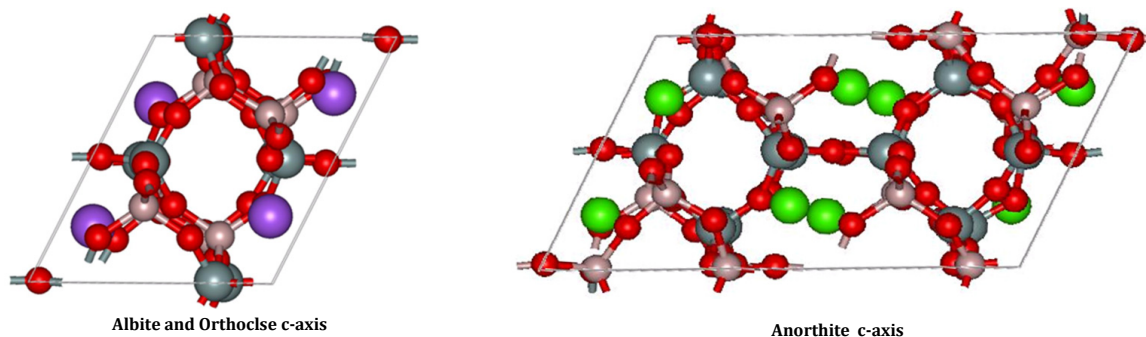


Figure 4. Representation of crystalline cells of Albite ($\text{NaAlSi}_3\text{O}_8$), Orthoclase (KAlSi_3O_8) and Anorthite ($\text{CaAl}_2\text{Si}_2\text{O}_8$), calculated from the Cerius database [26].

Table 1. Cell dimensions for albite, anorthite and orthoclase.

Cell dimensions	a, Å	b, Å	c, Å	α , °	β , °	γ , °
Albite	8.14	12.78	7.16	94.2	116.6	87.6
Anorthite	8.17	12.87	14.16	93.1	115.8	91.2
Orthoclase	8.62	12.99	7.19	90.0	116.0	90.0

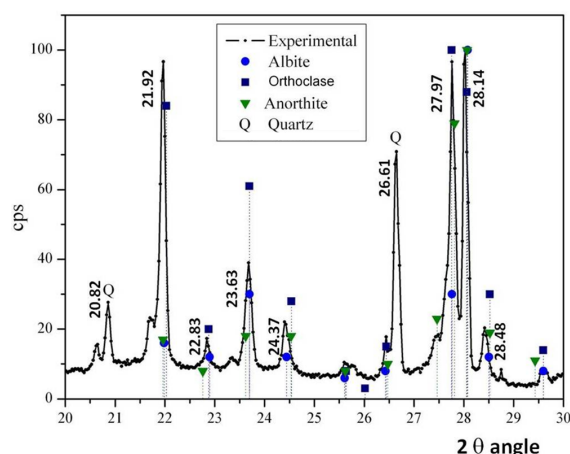


Figure 3. X-ray diffractogram of minerals in the vadose zone compared with albite, anorthite and orthoclase tectosilicates.

The diffraction of anorthite is slightly displaced from the main diffraction peaks of the mineral maybe due to the presence of twin cells. However, the three minerals have approximately the same crystallographic shape, which may result in similar sorption and physicochemical character.

Table 1 presents the cell dimensions of the minerals studied in this work. The length in a- and b-axis are very similar in the three cases. However, the length in c-axis is only similar in albite (7.16 Å) and orthoclase (7.19 Å), suggesting that they have isomorphous structures, but in anorthite this length is almost twice (14.16 Å).

The superficial area of particles was measured by the 20 points isotherm BET method giving $20.5 \text{ m}^2\text{g}^{-1}$. Hodgson analyzed the surface area of anorthite as function of dissolution rates and grain size, obtaining an area of approximately $1 \text{ m}^2\text{g}^{-1}$ [27]. In this work, the superficial area is 20 times higher. This could be one of the reasons for the uranium retention in the vadose layers mentioned before.

As the only structural difference of albite and orthoclase is the substitution of Na for K atoms, one way to study the participation of both tectosilicate minerals in the vadose layers is by analyzing their Na (representing albite), K (representing orthoclase) and Ca (representing anorthite) elemental content. This analysis was done by energy dispersive spectroscopy (EDS). The main elements found in the minerals were only

those participating in their chemical formulation: O, Na, Al, Si, K and Ca.

The elemental analysis showed that the atomic percent of K is 8.11% and the atomic percent of Ca is 9.83%, indicating that the abundance of orthoclase and anorthite in the vadose layers is similar, but much lower compared to the great participation of Na (albite), approximately 24% [28-30]. The rest of the composition is made up of other elements, O, Al and Si, common in the three tectosilicates. Considering these numbers, albite has approximately three times the content of orthoclase and 2.5 times the content of anorthite in the vadose layers studied in this work. However, it is important to note that anorthite has a double cell structure, which could result in approximately the same sorption effect as albite, due to its content.

3.4. Isoelectric point

As the tectosilicates studied in this work have similar crystalline structure, their individual isoelectric points should be very close. The pH isoelectric point of the composite mineral calculated by the mass titration techniques gives a $\text{pH}_{\text{iep}} = 8.06$, as shown in Figure 5.

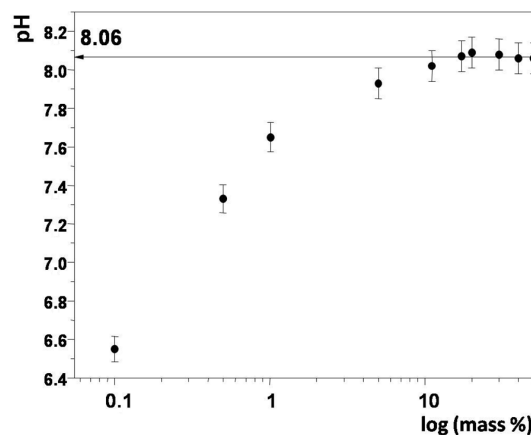


Figure 5. pH isoelectric point of the combined tectosilicate mineral.

3.5. Hydration time

Hydration time in sorption processes is very important because amphoteric surfaces need short contact time to retain particles or liquids before they spread into their surroundings. The surface-hydration analyses in this work were performed by acid/base potentiometric titrations. The acid or base consumption was plotted as a function of pH. The hydroxylated compounds were formed on the surface at pH near the

isoelectric point. The hydration time equilibrium was reached in approximately 1 hour. The hydration time for other minerals with structures composed by oxides or phosphates ranges from 6 to 24 h. [22,31].

3.6. Surface site density

Surface site density of minerals indicates superficial points that could be applied to retain particles or ions of another species, for example radionuclide content in nuclear leakages [31,32]. The surface site density of minerals in this work was calculated by comparing the acid consumption in the acid-basic titrations of aqueous mineral suspensions with one blank salt solution.

Figure 6 shows this comparison, the axes are presented in molar concentration. When the final part of the plots is linear, it can be assumed that no more reactions occur with the OH⁻ ions and the OH⁻ added are found in the solution as OH⁻ free. Subtracting these two values result the total OH⁻ taken by the solid phase. With this value, and considering the initial pH of titration and superficial area, the surface site density of the combined tectosilicates was calculated as 2.8 sites.nm⁻².

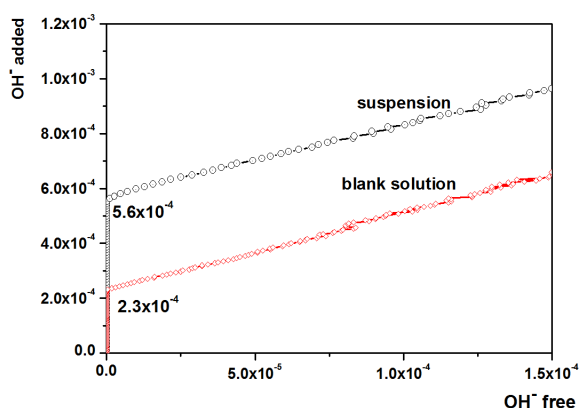
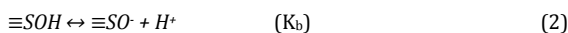
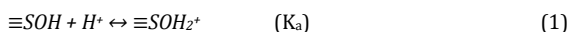


Figure 6. Comparison of OH⁻ moles added to the suspension versus the free OH⁻ moles in solution for a mineral suspension (circles) and the background salt (squares).

3.7. Acidity constants

The surface active sites ($\equiv\text{SOH}$) created during the hydration of minerals in solution were titrated to calculate the surface acidity constants. The superficial amphoteric species are dependent on the ground salt solution pH. The protonation and deprotonation equilibria can be described by modeling the acidity constants as follows.



$$K_a = \frac{[\text{SOH}_2^+]}{[\text{SOH}][\text{H}^+]} \exp(F\psi / RT) \quad (3)$$

$$K_b = \frac{[\text{SO}^-][\text{H}^+]}{[\text{SOH}]} \exp(-F\psi / RT) \quad (4)$$

where F is the Faraday constant, ψ the surface electrostatic potential, R the ideal gas constant, and T temperature expressed in Kelvin. K_a and K_b constants were calculated using experimental potentiometric titrations with FiteQL4 program applying the constant capacitance model (CCM) of the surface complexation theory. This model considers a low number of constraints and it is commonly used for high ionic strength conditions [23,27].

The modeling of the titration curve was performed to obtain K_a and K_b in the albite/orthoclase and anorthite found in the surface/solution interface in amphoteric conditions (Figure 7). Albite and orthoclase are treated as one compound because of their similar isomorphous structure. The total surface site density was used as the initial guess for the fitting procedure. The surface acidity constants and the total concentration of albite/orthoclase and anorthite is presented in Table 2.

Table 2. Surface acidity constants corresponding to albite/orthoclase and anorthite.

Mineral species	Log (K_a)	Log (K_b)	Total concent. (Mol/L)
Albite/Orthoclase	4.78711	-6.69198	6.696×10^{-4}
Anorthite	4.41696	-8.85619	1.745×10^{-3}

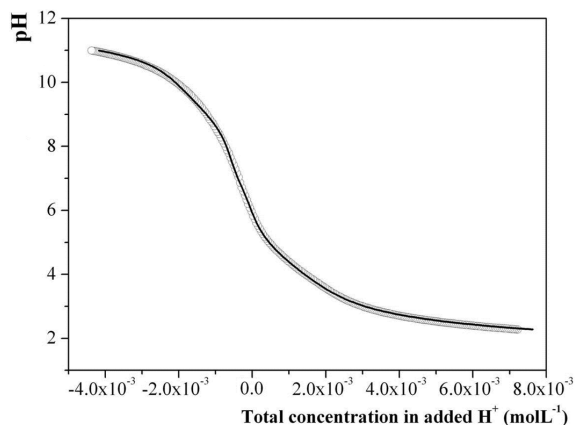


Figure 7. Acid-base titration of minerals in a 0.5 M potassium nitrate solution. Experimental (open circles) and CCM calculated (line) curves.

The distribution of the surface species versus pH is shown in Figure 8. The results indicate that the active sites concentration of anorthite is almost twice that of albite/orthoclase, probably because the longer c-axis cell dimension of anorthite develop an excess of active sites. With the distribution of species, the pH_{pie} specific for albite/orthoclase and anorthite can be obtained. The pH_{pie} calculated from titration fitted dataset was 5.6 for albite/orthoclase (XOH) and 6.7 for anorthite (YOH), as shown in Figure 8, which is more abundant and is near the pH of natural groundwater. Consequently, this factor may be responsible for the sorption of uranium on the surface.

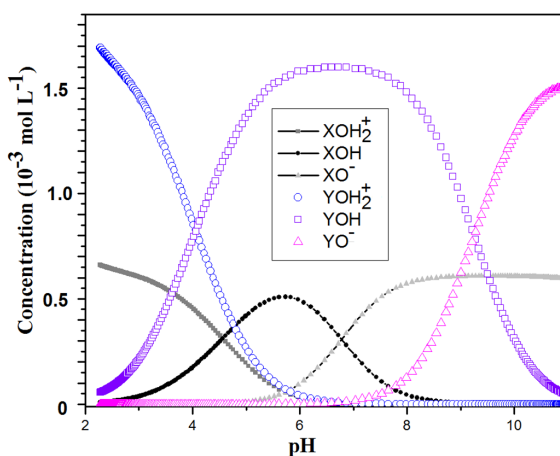


Figure 8. Species distribution diagram: Albite/orthoclase (Closed shapes) and Anorthite (Open shapes).

4. Conclusions

This study focused on identifying natural minerals in the vadose zone of an agricultural land with potential to retain uranium compounds. Crystallographic analysis showed that tectosilicate minerals such as anorthite ($\text{CaAl}_2\text{Si}_2\text{O}_8$), albite ($\text{NaAlSi}_3\text{O}_8$) and orthoclase (KAlSi_3O_8) were identified as the main components of that zone. Elemental analysis showed that albite was the main species in those tectosilicates. The active site concentration of anorthite is almost twice that of albite/orthoclase, probably due to the longer c-axis cell dimension of anorthite. The composite mineral has a specific surface area of $20.5 \text{ m}^2\text{g}^{-1}$ with site density of $2.8 \text{ sites nm}^{-2}$. These characteristics make this mineral a good candidate to capture uranium. The pH at the isoelectric point was 8.06, which allows reactions near the natural water pH. The optimal surface hydration time was reached in 1 h. It is very important to have amphoteric surfaces with a short contact time for sorption of uranium contaminants before they spread into their surroundings. The structural characteristics were used to calculate the surface acidity constants and the species distribution. The mineral species showed similar amphoteric behavior in presence of high ionic strength ground salt solutions. One of the advantages of these tectosilicates is that they are largely available as natural minerals in the soil.

Acknowledgements

We appreciate the support given in Scanning Electron Microscope analysis by Jorge Perez del Prado and Leticia Carapia for X-ray diffraction spectra.

References

- [1]. Kratz, S.; Schnug E.; Markel B. J.; Hasche-Berger A. (Eds.), Rock phosphates and P fertilizers as sources of U contamination in agricultural soils, Springer, Berlin, Heidelberg, 2006, pp. 57-68.
- [2]. Guzman, R. E. T.; Regil, O. E.; Alberich, E. M. V.; Hernandez, R. A.; Gutierrez, R. L. R.; Regil, O. E. *Water, Air, Soil Pollut.* **2006**, *175*, 77-98.
- [3]. Guzman, R. E. T.; Alberich, E. M. V.; Regil, O. E. *J. Radioanal. Nucl. Chem.* **2002**, *254(3)*, 509-517.
- [4]. DeMasily, G. *Radiochim. Acta* **1998**, *44-45*, 159-164.
- [5]. Grenthe, I. *Radiochim. Acta* **1991**, *52-53*, 425-432.
- [6]. Jaquier, P. *Radiochim. Acta* **1991**, *52-53*, 495-500.
- [7]. Dozol, M.; Hagemann, R. *Pure App. Chem.* **1993**, *65(5)*, 1081-1102.
- [8]. Guillaumont, R. *Radiochim. Acta* **1994**, *66-67*, 231-237.
- [9]. Day, D. H.; Hughes, A. E.; Leake, J. W.; Marples, J. A.; Marsh, G. P.; Rae, J.; Wade, B. O. *Rep. Prog. Phys.* **1985**, *48*, 1091-1154.
- [10]. Hueckel, T.; Peano, A. *Comput. Geotech.* **1987**, *3(2-3)*, 157-182.
- [11]. Abdelouahed, H. B.; Reguigui, N. *J. Radioanal. Nucl. Chem.* **2011**, *289*, 103-111.
- [12]. Guzman, R. E. T.; Rios, S. M.; Garcia, I. J. L.; Regil, O. E. *J. Radioanal. Nucl. Chem.* **1995**, *189(2)*, 301-305.
- [13]. Souka, N.; Shabana, R.; Farah, K. *J. Radioanal. Nucl. Chem.* **1976**, *33*, 15-23.
- [14]. Yinjie, S.; Hui, Z.; Qiaoling, Y.; Aimin, Z. *J. Radioanal. Nucl. Chem. Art.* **1995**, *198(2)*, 375-387.
- [15]. Lomenech, C.; Drot, R.; Simoni, E. *Radiochim. Acta* **2003**, *91*, 453-461.
- [16]. Regil, O. E.; Drot, R.; Simoni, E. *J. Colloid. Interface Sci.* **2003**, *263*, 391-398.
- [17]. Galambos, M.; Roszkopfova, O.; Kufcakova, J.; Rajec, P. *J. Radioanal. Nucl. Chem.* **2011**, *288*, 765-777.
- [18]. Garcia, G.; Ordoñez, E.; Drot, R.; Perez, M. *Inf. Tecnol.* **2004**, *15(4)*, 31-38.
- [19]. Zhang, Y.; Zhao, H.; Fan, Q.; Zheng, X.; Li, P.; Liu, S.; Wu, W. *J. Radioanal. Nucl. Chem.* **2011**, *288*, 395-404.
- [20]. Drot, R.; Lindecker, C.; Fourest, B.; Simoni, E.; *New J. Chem.* **1998**, *1*, 1105-1109.
- [21]. Hayes, K. F.; Redden, G.; Ela, W.; Leckie, J. O. *J. Colloid. Interface Sci.* **1991**, *142(2)*, 448-469.
- [22]. Noh, J.; Schwarz, J. J. *J. Colloid. Interface. Sci.* **1989**, *130*, 157-164.
- [23]. Herbelin, A.; Westall, J., FITEQL4 V 4.0 program; Report 96-01. Department of Chemistry, Oregon State University, Corvallis, 1996.
- [24]. Preocanin, T.; Kallay, N. *Croat. Chem. Acta* **1998**, *71(4)*, 1117-1125.
- [25]. Available at: <http://adsorption.org/awm/ads/EnCorr.htm> by Marczewski, A. W. Last update on: 01/04/2012.
- [26]. Cerius Database, Biosym/Molecular Simulations. USA, **1995**.
- [27]. Hodgson, M. E. *J. Geochem. Explor.* **2006**, *88*, 288-303.
- [28]. Armbruster, T.; Bürgi, H. B.; Kunz, M.; Gnos, E.; Brönnimann, S.; Lienert, C. *Am. Mineral.* **1990**, *75*, 135-140.
- [29]. Harlow, G.; Brown, G. E. Jr. *Am. Mineral.* **1980**, *65*, 986-995.
- [30]. Murakami, T.; Kogure, T.; Kadohara, H.; Ohnishi, T. *Am. Mineral.* **1998**, *83*, 1209-1219.
- [31]. Simoni, E., Encyclopedia of surface and colloid science, Marcel Dekker Inc. 2002.
- [32]. Appelo, C. A. J.; Postma, D. *Geochim. Cosmochim. Acta* **1999**, *63(19-20)*, 3039-3048.